Inherited human sex reversal due to impaired nucleocytoplasmic trafficking of SRY defines a male transcriptional threshold

Yen-Shan Chen[a], Joseph D. Racca[a], Nelson B. Phillips[a], and Michael A. Weiss[a,b,c,1]

Departments of [a]Biochemistry, [b]Biomedical Engineering, and [c]Medicine, Case Western Reserve University, Cleveland, OH 44106

Edited by Patricia K. Donahoe, Massachusetts General Hospital, Boston, MA, and approved August 14, 2013 (received for review January 16, 2013)

Human testis determination is initiated by SRY (sex determining region on Y chromosome). Mutations in *SRY* cause gonadal dysgenesis with female somatic phenotype. Two subtle variants (V60L and I90M in the high-mobility group box) define inherited alleles shared by an XY sterile daughter and fertile father. Whereas specific DNA binding and bending are unaffected in a rat embryonic pre-Sertoli cell line, the variants exhibited selective defects in nucleocytoplasmic shuttling due to impaired nuclear import (V60L; mediated by Exportin-4) or export (I90M; mediated by chromosome region maintenance 1). Decreased shuttling limits nuclear accumulation of phosphorylated (activated) SRY, in turn reducing occupancy of DNA sites regulating Sertoli-cell differentiation [the testis-specific SRY-box 9 (*Sox9*) enhancer]. Despite distinct patterns of biochemical and cell-biological perturbations, V60L and I90M each attenuated *Sox9* expression in transient transfection assays by twofold. Such attenuation was also observed in studies of V60A, a clinical variant associated with ovotestes and hence ambiguity between divergent cell fates. This shared twofold threshold is reminiscent of autosomal syndromes of transcription-factor haploinsufficiency, including XY sex reversal associated with mutations in *SOX9*. Our results demonstrate that nucleocytoplasmic shuttling of SRY is necessary for robust initiation of testicular development. Although also characteristic of ungulate orthologs, such shuttling is not conserved among rodents wherein impaired nuclear export of the high-mobility group box and import-dependent phosphorylation are compensated by a microsatellite-associated transcriptional activation domain. Human sex reversal due to subtle defects in the nucleocytoplasmic shuttling of SRY suggests that its transcriptional activity lies near the edge of developmental ambiguity.

organogenesis | sex determination | gonadogenesis | gene-regulatory network | protein-DNA interaction

The male phenotype in therian mammals is determined by *Sry* (1), a Y-chromosomal gene encoding an architectural transcription factor (TF) (2). SRY contains a central high-mobility group (HMG) box, a conserved motif of specific DNA binding and bending (Fig. 1*A*) (3, 4). Assignment of Sry as the testis-determining factor is supported by transgenic mouse models (5) and human mutations leading to gonadal dysgenesis with female somatic phenotype (Swyer syndrome) (6). Expressed in the pre-Sertoli cells of the differentiating gonadal ridge, Sry activates *Sox9*, an autosomal gene broadly conserved among vertebrate sex-determining pathways (7). Direct binding of Sry to specific DNA sites within the testis-specific core enhancer of *Sox9* (TESCO) activates a male-specific gene-regulatory network in the fetal gonadal ridge (7). Sustained *Sox9* expression orchestrates programs of cell–cell communication, migration, and differentiation leading to gonadogenesis (8), regression of the female primordia (following Sertoli-cell secretion of anti-Müllerian Hormone/Müllerian Inhibiting Substance; AMH/MIS) (9), and somatic virilization (through fetal Leydig-cell secretion of testosterone) (10). Mutations in this pathway are associated with disorders of sexual development (11).

Structure–function relationships in human SRY (hSRY) have been investigated through comparative biochemical and biophysical studies of Swyer variants (6). Most often arising de novo in spermatogenesis and clustering in the HMG box (Fig. 1*A*), such mutations typically impair specific DNA binding by direct or indirect perturbation of an angular protein–DNA interface (6, 12). The present study focuses on inherited mutations (V60L and I90M; asterisks in Fig. 1*A*) that by contrast allow near-native DNA binding and bending (13, 14). Such mutations are compatible with alternative developmental outcomes: testicular differentiation leading to virilization (fertile 46,XY father) or nascent ovarian differentiation leading to gonadal dysgenesis (sterile 46,XY daughter) (13). In the structure of the wild-type (WT) SRY–DNA complex (12), V60 and I90 pack within the minor and major wings (Fig. 1*B*) of the HMG box (consensus positions 5 and 35, respectively; Fig. 1*C*). The clinical substitutions each represent a subtle interchange of nonpolar side chains. Known inherited mutations in SRY are summarized in *SI Appendix*, Table S1.*

Inherited mutations in hSRY provide experiments of nature probing the threshold molecular properties of a developmental switch beyond DNA binding and bending. To this end, our studies exploited a model of the central SRY–*Sox9* regulatory axis (Fig. 1*D*) in a rodent fetal pre-Sertoli cell line (14–16). Our findings demonstrate that hSRY undergoes nucleocytoplasmic

Significance

Mutations in human *SRY* (sex determining region on Y chromosome) associated with somatic sex reversal provide a model for the perturbation of a genetic switch in organogenesis. Inherited alleles, associated with either testicular or ovarian differentiation, provide unique probes of threshold biochemical properties, defining mechanistic borders between functional and nonfunctional transcription factors. This study exploited two such alleles to demonstrate that bidirectional nucleocytoplasmic trafficking (import–export shuttling) enables robust operation of this switch via phosphorylation at a site external to the DNA-binding motif of the transcription factor. In accordance with studies of intersexual mice, our results suggest that human SRY functions at the edge of ambiguity.

Author contributions: M.A.W. designed research; Y.-S.C., J.D.R., and N.B.P. performed research; Y.-S.C., J.D.R., N.B.P., and M.A.W. analyzed data; and Y.-S.C. and M.A.W. wrote the paper.

The authors declare no conflict of interest.

This article is a PNAS Direct Submission.

[1]To whom correspondence should be addressed. E-mail: michael.weiss@case.edu.

This article contains supporting information online at www.pnas.org/lookup/suppl/doi:10.1073/pnas.1300828110/-/DCSupplemental.

*Seven inherited Swyer alleles of SRY have been reported (*SI Appendix*, Table S1). Analysis of specific DNA binding of one variant (V60L) by a gel mobility-shift assay provided apparent evidence for a severe impairment (>50-fold as estimated by absence of a shifted band) (53). Although this finding would imply a high transcriptional threshold (as so-marked a perturbation would seem required to render gonadogenesis ambiguous), these data are not in accordance with equilibrium-based measurement of the near-native properties of the variant HMG box (Table 1 and Ref. 14) and so presumably reflected accelerated dissociation of the variant complex during electrophoresis. Transcriptional activities of four other inherited variants were probed by reporter-gene cotransfection assays on overexpression in Chinese hamster ovarian cells but yielded a range of results (13), precluding assessment of an SRY transcriptional threshold.

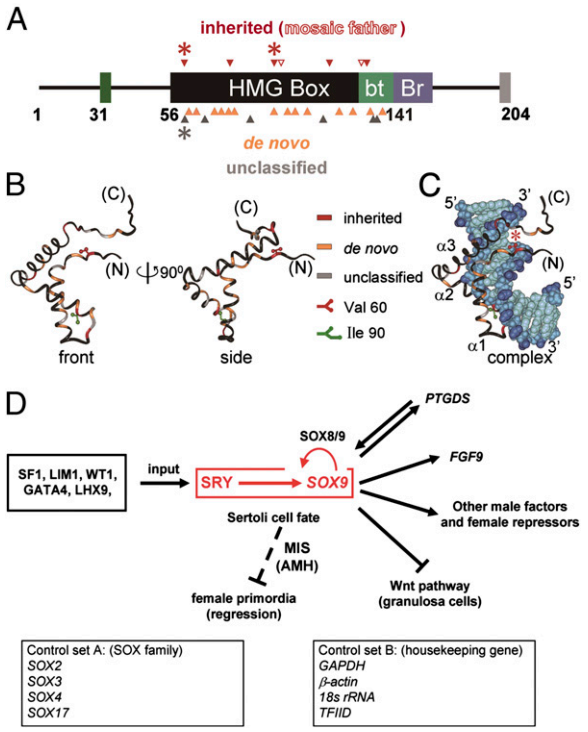

Fig. 1. Structure and function of human SRY. (*A*) Domain organization and Swyer mutations. Residues 56–141 comprise HMG box (black) and basic tail (bt; light green). Other domains: PKA phosphorylation sites (dark green), bridge domain (purple, Br), and PDZ-binding motif (gray). De novo, unclassified mutations (amber and gray triangles, respectively), inherited mutations (filled red triangles), and mosaic fathers (open red triangles) are shown. Asterisks indicate V60L (red), V60A (gray), and I90M (red). (*B–D*) Structure of hSRY and outline of SRY-*Sox9* regulatory axis. (*B*) Ribbon model of hSRY HMG box (front and side views; color code at right). V60 and I90 (balls and sticks) are highlighted in red and green. (*C*) hSRY (ribbon)-DNA (CPK model) complex. HMG color code is as in *A*; DNA atoms are light blue (bases), medium blue (deoxyribose), or dark blue (phosphodiester linkages). The minor wing comprises N-terminal β-strand and C-terminal segment of α-helix α3; the major wing contains α1, α2, and N-terminal portion of α3. Asterisk indicates minor wing minicore containing V60 (red balls and sticks). (*D*) SRY→*SOX9* regulatory axis (red box) with genetic inputs (box at left) and outputs to a male-specific gene-regulatory network (→) leading to inhibition of granulosa-cell fate (solid ⊥), and Müllerian regression (dashed ⊥). Red curved arrow indicates SOX8/9-mediating feedback maintaining *SOX9* expression. FGF9, fibroblast growth factor 9; GATA4, GATA binding protein 4; LHX9, LIM homeobox 9; LIM1, homeobox protein Lhx 1; MIS (AMH), Müllerian Inhibiting Substance (Anti-Müllerian Hormone); PTGDS, Prostaglandin D2 synthase; SF1, steroidogenic factor 1; WT1, Wilms' tumor 1; Wnt, wingless-type. Boxes at *Lower* indicate sex-independent *SOX* family genes (*Left*) and housekeeping genes (*Right*).

shuttling (NCS) and that such NCS is coupled to an activating N-terminal serine phosphorylation (17, 18). Respective V60L and I90M variants exhibit selective impairment of nuclear import (as mediated by Exportin-4) or nuclear export (mediated by CRM1) but otherwise retain substantial gene-regulatory activity in accordance with the phenotypes of the fathers. Mutational impairment of NCS in either direction reduces nuclear accumulation of phosphorylated hSRY, in turn attenuating SRY-dependent transcriptional activation of *Sox9* in accordance with the phenotypes of the XY daughters. Although NCS-dependent transcriptional regulation is likely to be broadly conserved among *Sox* genes (*SI Appendix*, Table S2) (19, 20), its importance to the function of SRY has been obscure in studies of mouse models (21). In a recent study (22) we demonstrated that murine Sry fails to undergo NCS as a consequence of an inactive nuclear export signal (NES) motif. Whereas the HMG box of hSRY contains an active NES (IxxxLxxxxx**M**L), microsatellite-associated rodent variants contain the variant sequence IxxxLxxxxx**S**L (22). Such variation is associated with clade-specific insertion of a DNA microsatellite in the divergent evolution of the Y chromosome in superfamily *Muroidea* (order *Rodentia*) (23).

Mammalian TFs regulating tissue- and stage-specific gene expression are ordinarily present at low abundance (1-100 nM representing 10^2 to 10^4 molecules per nucleus) (24). Studies in cell culture, however, often use strong viral promoters (such as that derived from the cytomegalic virus) (25), which typically confer high-level TF expression (1-10 μM representing 10^5 to 10^6 molecules per nucleus). Because such overexpression can alter quantitative patterns of gene expression and qualitative biological responses (26), the contribution of NCS-linked phosphorylation to the transcriptional activity of hSRY was estimated at progressively lower levels of protein expression within the physiological range. In each case, the limiting extent of attenuation was twofold, a quantitative threshold reminiscent of disorders of sexual development-associated syndromes of autosomal transcription-factor haploinsufficiency (11). An analogous Sry-related threshold in XY mice has been inferred based on studies of intersexual phenotypes due to the strain-specific phenomenon of Y chromosome/autosome incompatibility (27–29). This seeming paradox of mice and men highlights the tenuous beginning of the male program (11). Defining a critical boundary between testicular self-organization and gonadal dysgenesis, inherited human sex reversal associated with subtle perturbation of hSRY thus violates the principle of Waddington canalization (30). Whereas the latter emphasizes the importance of robustness in developmental pathways (31), we speculate that SRY has evolved to the edge of ambiguity as a developmental mechanism to ensure male phenotypic variation in social mammals.

Results

Our studies primarily used rat embryonic pre-Sertoli XY cell line CH34 (16). We previously described a transient-transfection assay of hSRY-directed transcriptional activation of endogenous *Sox9* (14). Using quantitative PCR [real-time-Q-rtPCR (qPCR)], this assay measures the time-dependent accumulation of mRNAs in a downstream gene-regulatory network (32). *Sox9* expression was measured following transient transfection of WT or mutant *SRY* constructs. Although use of a cytomegalovirus (CMV) promoter under standard transfection conditions yielded ~10^5 to 10^6 molecules per transfected cell, such overexpression could be attenuated by dilution of the plasmid with an empty vector to achieve an appropriate TF concentration (10^2 to 10^4 molecules per cell).[†] A subset of key findings was replicated in a human male cell line.

Inherited mutations of sexual development in hSRY (V60L and I90M; first and second red asterisks in Fig. 1*A*, respectively) were chosen based on their compatibility with native-like structure and DNA binding (Table 1) (14). Structural environments are shown in Fig. 1 (12). Conserved as Val among mammalian SRY/Sry domains, V60 (consensus position 5 in the minor wing) adjoins a bipartite nuclear localization signal (NLS). A second mutation at this site (V60A; father uncharacterized) was associated with ovotestes (33). V60L and V60A do not affect box stability and permit DNA-dependent folding of the minor wing with near-native DNA bending (14). I90 projects from the second α-helix (α2) into the major-wing core as part of an aliphatic motif (I90, L94, M100, and L101; consensus positions 35, 39, 45, and 46) proposed to function as a Sox nuclear export signal (NES) (19, 20). Although I90M destabilizes the free box (ΔT_m 4 °C and $\Delta\Delta G_u$ 0.5 kcal/mole) (Table 1 and *SI Appendix*, Fig. S1), near-native specific DNA affinity (K_d) and DNA bending are nonetheless maintained (Table 1 and *SI Appendix*, Figs. S2 and S3). Like V60L and V60A box–DNA complexes (14), the I90M

[†]Level of hSRY expression was estimated by anti-HA Western blot in relation to Western analysis of control proteins α-tubulin (*SI Appendix*, Fig. S14).

Table 1. Properties of SRY Variants

SRY variant*	K_d, x 10^{-9} M	θ†	T_m, °C‡	$\Delta\Delta G_u$, kcal/mol§	Relative *Sox9* mRNA accumulation¶ Assay A	Assay B	Assay C
Wild type	14 ± 3	74°	40	—	100 ± 4	100 ± 4	100 ± 6
V60A	27 ± 5	72°	40	0.1 ± 0.1	42 ± 9	93 ± 8	98 ± 6
V60L	32 ± 2	71°	40	0.1 ± 0.1	47 ± 9	89 ± 7	92 ± 5
I90M	15 ± 1	74°	36	0.5 ± 0.1	43 ± 8	42 ± 9	46 ± 5

*Biophysical studies used the isolated HMG box; qPCR studies used full-length HA-tagged SRY. FRET-based estimates of dissociation constants (K_d) revealed a small decrease in affinity of V60A and V60L domains relative to wild type whereas that of I90M was unchanged. Stopped-flow FRET studies of protein–DNA dissociation demonstrated that respective dissociation-rate constants (k_{off}) of V60L, V60A, and I90M domains are increased [k_{off} 0.24(± 0.008) s^{-1}, 0.17(±0.005) s^{-1}; and 0.14(±0.001) s^{-1}, respectively] relative to wild type [0.033(±0.001) s^{-1}; see ref. 14 and SI Appendix, Fig. S2].

†DNA bend angles were investigated by permutation gel electrophoresis; uncertainties were ±1° (14). V60A and V60L values are from Phillips et al. (14); I90M value is from Knower et al. (13).

‡Midpoint unfolding temperatures were based on CD (4).

§Differences in free energies of unfolding ($\Delta\Delta G_u$), with reference to WT (—), were estimated as described (14); WT ΔG_u is 3.8(±0.1) kcal/mole.

¶Values of *Sox9* mRNA accumulation were at low plasmid dose (50-fold dilution) (Fig. 2) to avoid effects of overexpression. Assay A provides baseline values in the absence of SV40 NLS or proteosome inhibition. Assay B, effects of fused SV40 NLS. Assay C, effects of NLS/MG132 double rescue.

complex exhibits a reduced kinetic lifetime with compensating changes in on-rate constants similar to wild type.

Transcriptional Regulation in a Pre-Sertoli Cell Model. CH34 cells were used to probe hSRY-dependent activation of *Sox9*; transfection efficiency was 32.6 (± 1.2) percent as inferred from control cotransfection of a plasmid encoding green fluorescent protein (GFP). Transient transfection of WT hSRY under standard conditions (1 μg per well) activated expression of *Sox9* by eightfold relative to an empty vector (black bar in Fig. 2*A*). Extent of transcriptional activation decreased to fivefold on successive dilution of the hSRY plasmid by the empty vector (maintaining total transfected DNA constant) to a final dilution of 0.02 μg of hSRY plasmid and 0.98 μg of empty vector per well (50-fold dilution; white bar in Fig. 2*A*). Such dilution provided a control for overexpression artifacts.‡

Although *Sox9* is the principal target of Sry (7), additional qPCR assays were undertaken to characterize a downstream gene-regulatory network in relation to in situ transcriptional profiling of the murine XY gonadal ridge (28). Whereas transient expression of hSRY did not affect mRNA accumulation of non–sex-related *Sox* genes and housekeeping genes (boxes at *Lower* in Fig. 1*D*), specific up-regulation of *Sox8*, *Sox9*, *fibroblast growth factor 9* (*Fgf9*), and *prostaglandin D2 synthetase* (*Ptgd2*) were observed in accord with their known roles in testicular differentiation (34). No such changes in mRNA accumulation were observed on transient transfection of an empty plasmid or a control plasmid expressing a stable hSRY variant devoid of specific DNA-binding activity (I68A) (35). Further, following 24-h incubation in serum-rich medium, no significant changes were observed in the expression of rat *Sry* itself.

Activities and Stabilities of hSRY Variants. Comparative studies of variant hSRY constructs (V60L, V60A, and I90M) demonstrated that (*i*) the two minor-wing substitutions exhibited decreased transcriptional activity at each dilution tested whereas (*ii*) major-wing substitution I90M enhanced *Sox9* expression when overexpressed but exhibited progressive loss of function with serial dilution (at right in Fig. 2*A*). Remarkably, at highest dilution (50-fold; white bars in Fig. 2*A*), the three substitutions were each associated with twofold loss of *Sox9* activation relative to wild type at the same dilution. These trends were also observed in the downstream gene-regulatory network modulated by the SRY-*Sox9* axis (*SI Appendix*, Fig. S4). The anomalous dilution-related properties of I90M hSRY motivated assessment of proteolytic stability and cellular NCS as factors that could lead to overexpression artifacts.

Cellular turnover of hemagglutinin (HA)-tagged hSRY constructs (transfected without dilution) was evaluated following cycloheximide inhibition of translation (Fig. 2*B*). Comparison of anti-HA Western-blot intensities demonstrated that V60L and V60A variants are more susceptible to degradation than are WT or I90M hSRY (graph in Fig. 2*B*). Such differential degradation could be circumvented through addition of proteosome-inhibitor MG132 (*SI Appendix*, Fig. S5). Subcellular localization was investigated using immunofluorescence microscopy (Fig. 2*C*); control GFP cotransfection studies demonstrated that WT and variant constructs achieved similar transfection efficiencies; 900 cells were counted in each case (triplicate by blinded coworkers). Representative images are shown in Fig. 2*C, Lower* in relation to corresponding nuclear staining of the same cells with 4',6-diamidino-2-phenylindole (DAPI) (Fig. 2*C*, *Upper*). The variant proteins exhibited contrasting perturbations relative to wild type (Fig. 2*D*). Whereas V60L and V60A often exhibited pancellular distributions with significant reduction in exclusive nuclear staining (gray bars in Fig. 2*D*), I90M hSRY exhibited a reduced pancellular fraction (white bars in Fig. 2*D*) with increase in exclusive nuclear staining. Partial restoration of nuclear localization of V60L and V60A hSRY was achieved by N-terminal fusion of an exogenous nuclear localization signal (NLS) derived from SV40 large T Antigen (36) ("+NLS" at right in Fig. 2*D*). No significant changes in nuclear accumulation of WT hSRY were observed in control studies of NLS-hSRY (*SI Appendix*, Fig. S6); I90M NLS-hSRY was not tested.

Immunofluorescence studies were repeated on addition of MG132 after 24-h posttransfection (Fig. 2*E*). As expected, proteosomal inhibition did not affect nuclear localization of WT or I90M hSRY (Fig. 2 *D* and *E*). In the absence of the fused NLS, MG132 treatment led to small decreases in extent of residual GFP-positive cells lacking detectable hSRY expression (100-sum of gray and white bars in Fig. 2 *D* and *E*); this trend did not achieve statistical significance. Strikingly, the combination of MG132 treatment and SV40 NLS fusion led to near-complete rescue of nuclear localization of V60L and V60A hSRY (right-hand bars in Fig. 2*E*; for representative cellular images see Fig. 2*C*). The efficiency of NLS/MG132 "double rescue" motivated reinvestigation of the functional properties of V60L and V60A hSRY under conditions wherein WT and variant proteins were expressed at similar levels and with similar patterns of subcellular localization (Fig. 2*F*). Whereas NLS fusion and/or addition of MG132 had no significant effects on transcriptional activation of *Sox9* by WT or I90M hSRY at any dilution, defective activation of *Sox9* by V60L or V60A hSRY was partially overcome by either maneuver, and double rescue led to native-like *Sox9* expression (Fig. 2*F*, *Right*).

Chromatin immunoprecipitation (ChIP) studies were undertaken of SRY/Sry binding sites in the TESCO element of *Sox9* (Fig. 3*A*, with primer sets defined in Fig. 3*B*; ref. 7). Occupancy (as probed by ChIP band intensities relative to input controls following transfection without plasmid dilution) of I90M hSRY

‡Our finding that I90M attenuates SRY function at an appropriate level of TF expression (10^2 to 10^4 protein molecules per nucleus) stands in disagreement with cotransfection studies using a reporter gene (*luciferase*) under the control of a human TES element (13). The latter studies demonstrated enhanced transcriptional activity of I90M SRY under conditions of its CMV promoter-driven overexpression in a Chinese hamster ovarian cell line (presumably due to enhanced nuclear accumulation) in accordance with the present studies in CH34 and PC-3 cells in the absence of plasmid dilution (Fig. 2 and *SI Appendix*, Fig. S12). We have also replicated the findings of ref. 13 in NT2-D1 cells following cotransfection of *luciferase* under the control of the minimal mouse TESCO element (SI Appendix, Fig. S15). In this cell line, the protocol of Knower and colleagues (13) leads in our hands to expression of ~1.5 million epitope-tagged SRY molecules per cell (*SI Appendix*, Fig. S16).

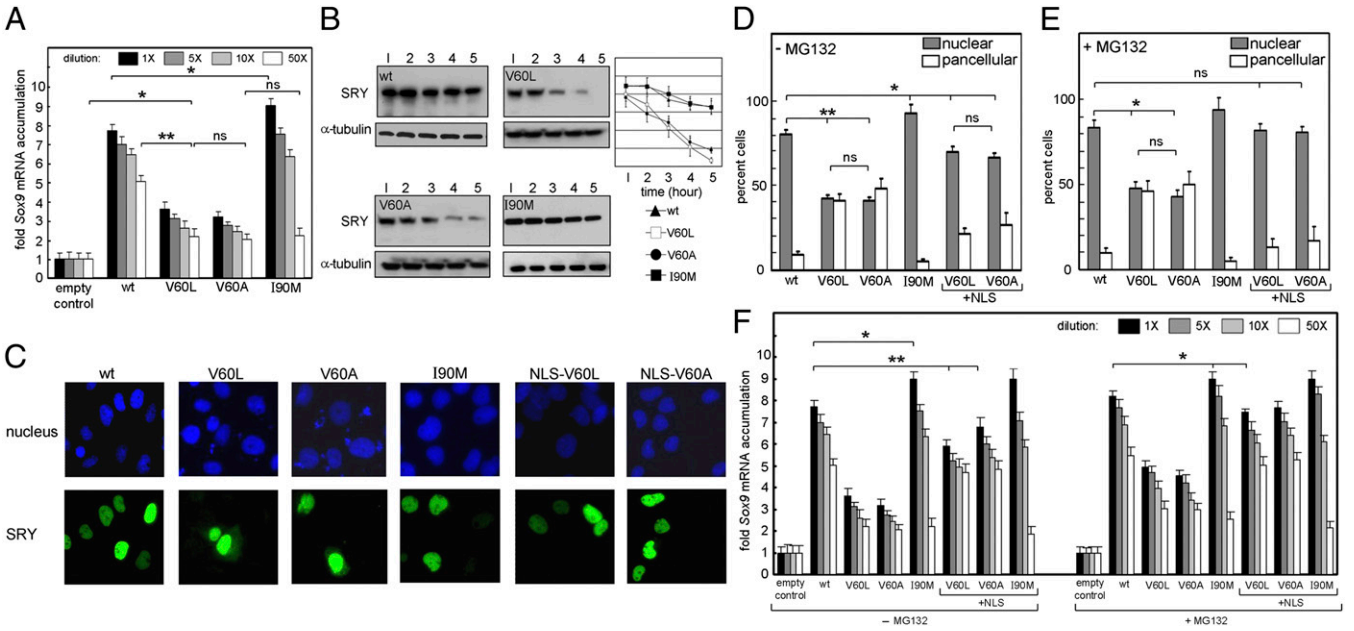

Fig. 2. Transcriptional activity and nuclear localization. (*A*) Dependence of *Sox9* expression on dose of transfected hSRY plasmid: 1 μg (black), 0.2 μg (dark gray), 0.1 μg (medium gray), 0.02 μg (white); total transfected DNA was the same. Brackets designate *P* values (*) <0.05 or (**) <0.01; "ns" indicates *P* values > 0.05. (*B*) Cycloheximide assay. Proteolysis is enhanced by V60L and V60A but unaffected by I90M. Gels are at *Left*. Graph at *Right* depicts hSRY degradation following inhibition of protein synthesis. (*C*) Subcellular localization of epitope-tagged SRY: DAPI nuclear staining (*Upper* row blue) and SRY (*Lower* row green). V60L and V60A SRY are pancellular; nuclear accumulation was rescued by SV40 NLS (*Right*). I90M augments nuclear localization. Images were obtained following MG132 treatment. (*D* and *E*) Histograms describing nuclear (gray) and pancellular (white) patterns in absence (*D*) or presence (*E*) of MG132. Gray and white bars sum to <100 due to occasional GFP-positive cells lacking SRY. SRY was at highest dose in *A*. Brackets indicate statistical comparisons. "+NLS" indicates rescue by SV40 NLS. I90M augments nuclear localization under all conditions tested. (*F*) Relationship between *Sox9* expression and hSRY dose. qPCR data were obtained in absence (*Right*) or presence (*Left*) of MG132. Within each set, additional data were obtained with fused SV40 signal (+NLS). At lowest dose of V60L or V60A, rescue of *Sox9* expression required only fused NLS. I90M hSRY at higher doses was superactive; plasmid dilution unmasked a twofold defect unaffected by fused NLS or MG132.

was indistinguishable from wild type (lanes 5 and 6 in Fig. 3*C*; see also *Lower* histogram). Control studies of inactive I68A hSRY (35) demonstrated an absence of enhancer binding; further control studies used de novo clinical mutants R62G and R75N in the N-terminal bipartite NLS of the HMG box (37). R62G and R75N (which impair both NLS1 specific DNA binding) demonstrated weak ChIP band intensities (Fig. 3*C*, lanes 1 and 2 in gel panel and the *Lower* histogram). Whereas TESCO-specific ChIP band intensities for V60L and V60A hSRY in the absence of NLS/MG132 were reduced to *ca.* half of the WT level (Fig. 3*C*), double rescue restored near-native enhancer occupancy (Fig. 3*D*). As in the *Sox9* qPCR assay, double-rescue of V60A hSRY was more complete than that of V60L hSRY (set c in Fig. 3*D*). These findings imply that the minor-wing variants, once bound to the *Sox9* enhancer, retain native-like gene-regulatory properties in a cellular milieu in accordance with their native-like biophysical properties (14).

Analysis of hSRY Protein–Protein Interactions. The above findings motivated investigation of how the mutations affect binding of hSRY to the NCS machinery. V60L and V60A adjoin the N-terminal bipartite basic NLS of the HMG box (21); this motif (residues 61–77 of hSRY; **KR**PMNAFIVWSRDQ**RRK**; basic residues in bold) binds to Exportin-4 (Exp4) to mediate nuclear import (37) rather than importin-α or -β (38). Coimmunoprecipitation (co-IP) studies were thus undertaken based on co-transfection of HA-tagged hSRY and FLAG-tagged Exp4 (Fig. 4*A*). The studies revealed that, whereas I90M mutation does not affect binding to Exp4 (lanes 1 and 6 in Fig. 4*B*), a graded series of perturbations were observed among the other variants (lanes 2–5). Measurement of relative band intensities (in triplicate) (*SI Appendix*, Fig. S7) defined the order V60L [mildest impairment; 60(±13)% relative to WT hSRY] and V60A [41(±13)%] relative to control mutations R75N [23(±6)%] and R62G [most severe; 17(±7)%] as previously characterized (37).

Nuclear export of SOX proteins is mediated by CRM1 via a conserved NES in the HMG box (20). Binding of hSRY (NES consensus IxxxLxxxxx**ML**; residues 35–46 in the consensus HMG box) to endogenous CRM1 was demonstrated in CH34 cells by co-IP (lane 7 in Fig. 4*C*). Analogous CRM1-dependent NCS was observed in studies of goat Sry and deer Sry, whose HMG boxes bear active NES variant IxxxLxxxxx**RL** (*SI Appendix*, Fig. S8). Binding of hSRY to CRM1 was unaffected by V60L or V60A (lanes 9 and 10 in Fig. 4*C*) but markedly impaired by I90M (lane 8) in accordance with its enhanced nuclear accumulation. Binding of hSRY to CRM1 and resulting NCS were also impaired by mSry-related substitution IxxxLxxxxx**SL** and by multiple Ala substitutions (AxxxAxxxxxAL) (*SI Appendix*, Fig. S9). Mutation-specific perturbations of hSRY–Exp4 or hSRY–CRM1 interactions stand in contrast to the absence of perturbations in assays of hSRY–calmodulin (CaM) binding. Although such binding (mediated by the N-terminal segment of the hSRY HMG box) has been proposed to direct nuclear entry (38), co-IP studies of endogenous CaM (outlined in Fig. 5*A*) revealed similar levels of binding to diverse mutations in the HMG box, including V60L and V60A (Fig. 5 *B* and *C*). Biochemical and biophysical studies of V60L and V60A hSRY–CaM complexes likewise demonstrated similar affinities and structural features (*SI Appendix*, Fig. S10).

Protein–protein interactions involving SRY have also been implicated in male-specific inhibition of Wnt/β-catenin signaling (Fig. 5*D*) (39). Such signaling is operative in ovarian development, and its inappropriate activation in the XY gonadal ridge (via stabilization of β-catenin) can be associated with human sex reversal (40). Although in pre-Sertoli cells this pathway is not well characterized, a functional SRY assay has been described in nongonadal

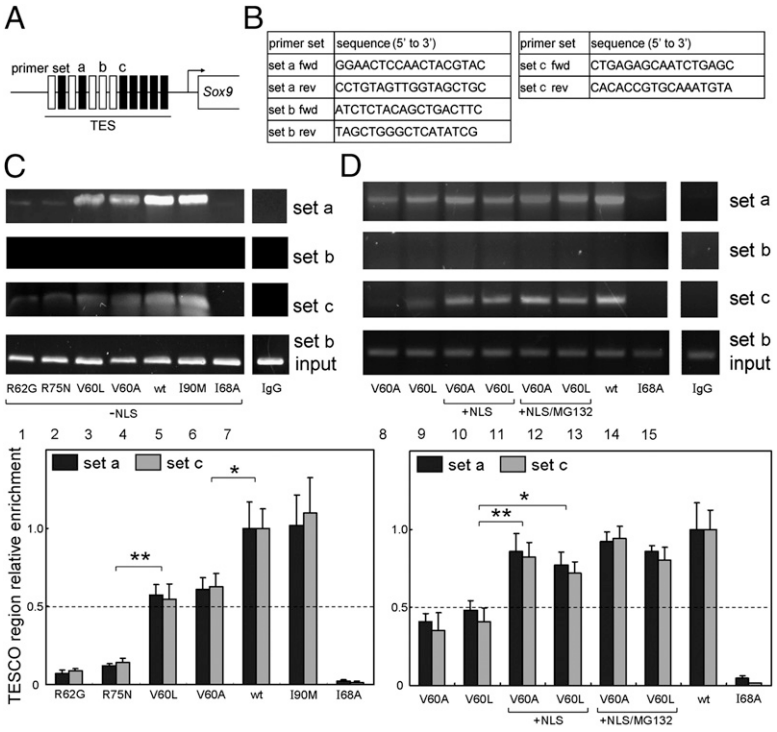

Fig. 3. ChIP assays and interactions of hSRY with nuclear import–export machinery. (*A–D*) ChIP assays probing SRY occupancy of target sites within *Sox9* testis-specific enhancer core element (TESCO). (*A*) TESCO fragment boxes (black, with SRY binding sites; and white, sites with no detectable binding). (*B*) Primer sets a and c probed for SRY occupancy; primer set b provided negative control. (*C*) Histogram and representative gel show results of ChIP of variants. Gel showing results of ChIP of variants without NLS rescue. R62G and R75N are de novo clinical mutations in the N-terminal bipartite NLS of the HMG box and in part impair specific DNA binding. (*D*) Histogram and representative gel showing ChIP studies of variants with NLS/MG132 rescue: lanes 8 and 9, without rescue; lanes 10 and 11, NLS fused; lanes 12 and 13, NLS/MG132 double rescue; lane 14 and 15, positive and negative hSRY controls, respectively. At *Right* are nonspecific IgG controls.

and germ-cell lines (39). This assay was adapted to CH34 cells stably transfected to express activated β-catenin variant S37A and transfected by a chimeric SRY construct (hSRY residues 1–155 and mouse Sry residues 128–396 as above); a functional read-out was provided by luciferase under the control of a β-catenin–responsive promoter (TOPflash; Fig. 5*E*). Transient transfections were performed with 50-fold dilution of SRY plasmids to minimize overexpression and in the presence of MG132 to equalize protein levels. Comparison of the CH34 cells expressing S37A β-catenin with the parent cell line revealed a 40-fold increase in luciferase activity (lanes 1 and 2 in Fig. 5*F*). This activity was inhibited by 3.5-fold on transient transfection of an SRY chimera bearing the WT human HMG box ("WT" in Fig. 5*F*, lane 3). Inhibition required specific DNA binding as demonstrated by maintenance of luciferase activity on transient transfection of SRY chimeras bearing inactive control mutations I68A or G95R (lanes 7 and 8 in Fig. 5*F*). Inherited mutations V60L and I90M as well as ovotestis-associated mutation V60A gave rise to intermediate levels of luciferase activity (lanes 4–6 in Fig. 5*F*). Whereas NLS fusion did not affect the inhibitory activity of the I90M construct (lanes 6 and 11 in Fig. 5*F*), partial rescue of nuclear localization enabled the V60L and V60A constructs to achieve near-native inhibition of luciferase activity (lanes 9 and 10).

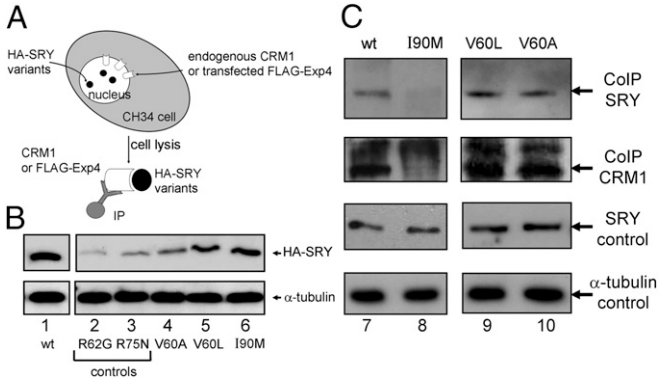

Fig. 4. Molecular mechanisms of nucleocytoplasmic shuttling. (*A*) Schematic outline of CRM1 and Exp4 co-IP assays. (*B* and *C*) Biochemical studies of the binding of epitope-tagged hSRY variants to nuclear import (Exp4) or nuclear export machinery (CRM1). Internal loading controls are provided by α-tubulin (*Bottom*). (*B*) Exp4 co-IP assay. Whereas the de novo mutations in the N-terminal NLS exhibit marked impairment, V60L exhibits only mild impairment, and V60A intermediate; no defect was observed for I90M. (*C*) CH34 CRM1 co-IP assay. Mutations at position 60 did not impair binding to CRM1; I90M causes almost complete lack of binding.

Nuclear Trafficking Affects hSRY Phosphorylation. SRY in primates contains potential phosphorylation sites N-terminal to the HMG box (hSRY residues 29–36; RRSSSFLC) recognized by protein kinase A (PKA); phosphorylation augments specific DNA binding (17). To investigate whether altered NCS affects phosphorylation of hSRY (HA-tagged) and thus enhancer binding, we evaluated by co-IP the extent of phosphorylation in cytosolic and nuclear fractions; an anti-phosphoserine antiserum was used to pull down phosphoproteins for Western blot by anti-HA antiserum (Fig. 6*A*). Molecular markers for fidelity of fractionation were provided by glyceraldehyde-3-phosphate dehydrogenase (GAPDH; cytosol) and Ying-Yang 1 (YY1; nucleus) as shown in Fig. 6*B, Bottom*. Epitope-tagged hSRY variants containing PKA-site substitutions RRAAAFL ("phospho-dead") or RRDDDFL ("phospho-mimic") were not detected as further described in a recent study (22); these findings indicate that, in CH34 cells, this is the only site of serine phosphorylation (green box in Fig. 6*C*). Studies were conducted following 50-fold dilution of the hSRY plasmid and in the presence of MG132. Because of the low uniform levels of hSRY expression under these conditions, each assay required pooling extracts from fifteen 10-cm plates grown to confluence.

As expected, WT hSRY was detected predominantly but not exclusively in the nuclear fraction (lanes 1 and 5 in Fig. 6*B*). The extent of phosphorylation was similar in the two fractions as indicated by the ratio of band intensities in Fig. 6*B*, *Top* (phospho-hSRY) to band intensities beneath (total HA-tagged hSRY). Also in accordance with the results of immunofluorescence microscopy (above), I90M hSRY exhibited increased nuclear accumulation (lanes 2 and 6 in Fig. 6*B*). Strikingly,

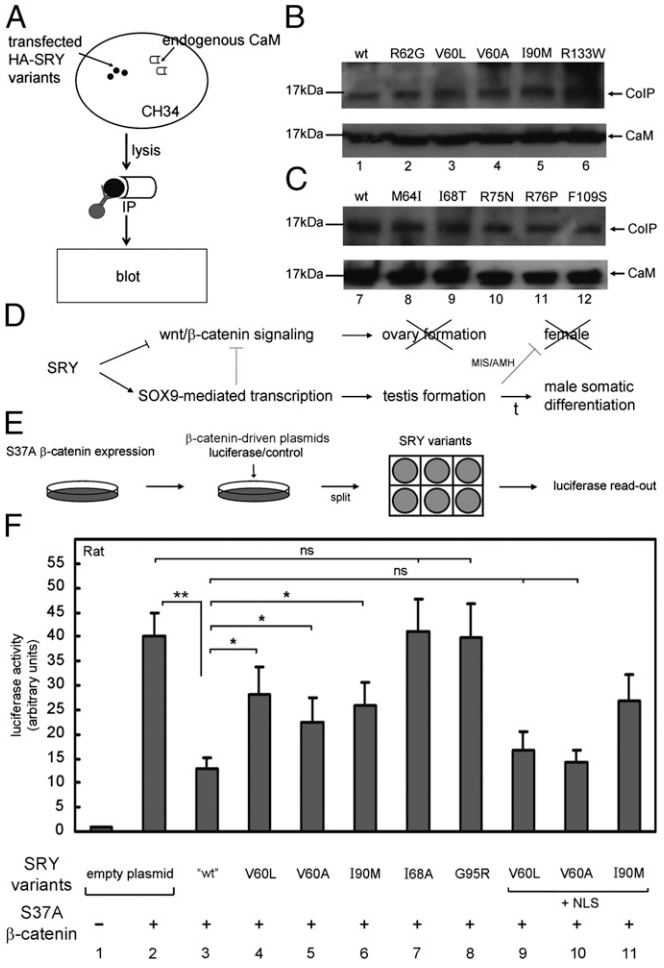

Fig. 5. Calmodulin binding and Wnt signaling. (*A–C*) hSRY binding to CaM. (*A*) Design of co-IP assay using transfected HA-tagged SRY variants. Complexes were analyzed by SDS/PAGE immunoblotted with anti-CaM antiserum. (*B* and *C*) Western blots documenting similar CaM binding in WT and variant complexes; differences were not statistically significant. Results were normalized by CaM immunoblotting (*Lower*). Control studies using other de novo mutations at positions 62, 64, 68, 75, and 76 lie within the CaM-binding motif; position 109 lies on the back side of the major wing; and 133 lies within the C-terminal NLS. (*D*) Male gonadal ridge (left) requires positive and negative regulatory steps (↓ and ⊥, respectively) to activate the testicular program (SOX9-dependent) and repress the ovarian program (Wnt/β-catenin pathway). Dotted interactions designate cross-talk; "X"s indicate absence of ovaries and female somatic differentiation; and "t" designates testosterone-dependent virilization. (*E*) Wnt/β-catenin reporter-gene assay. Cells were split and cotransfected by WT or variant SRY plasmids to enable luciferase read-out. (*F*) Histogram summarizing Wnt/β-catenin repression assay performed at the lowest plasmid dose (50-fold dilution as defined in Fig. 2). MG132 was added to ensure equal levels of protein expression. Repression relative to WT SRY was in part relieved by inherited mutations V60L, V60A, and I90M. The repression-related activity of V60L and V60A was almost fully restored by fused NLS. Full relief was observed in control studies using substitution I68A and de novo mutation G95R (which block specific DNA binding) (4, 53). Brackets designate statistical comparisons as in Fig. 2.

however, the total phosphorylation and relative phosphorylation of I90M hSRY were decreased in the nucleus despite its enhanced accumulation in that fraction. The twofold reduction in *Sox9* transcriptional activation observed under these conditions (50-fold plasmid dilution) presumably reflects a defect in phosphorylation, which more than offsets any increase in transcriptional-regulatory activity that would otherwise be associated with its enhanced nuclear accumulation. V60L and V60A hSRY were predominantly detected in the cytosolic fraction in accordance with impairment of nuclear entry (Fig. 6*B*, comparison of lanes 3 and 4 with lanes 7 and 8, respectively). Whereas the relative extent of phosphorylation in the cytosolic fraction is similar to that of WT hSRY, a striking reduction was observed in each case in the absolute amount of phosphorylated protein in the nuclear fraction (lanes 7 and 8 in Fig. 6*B, Top*).

To investigate the relationship between N-terminal phosphorylation of hSRY and transcriptional activation of *Sox9*, phospho-dead and phospho-mimic variants (Fig. 6*C*) were used

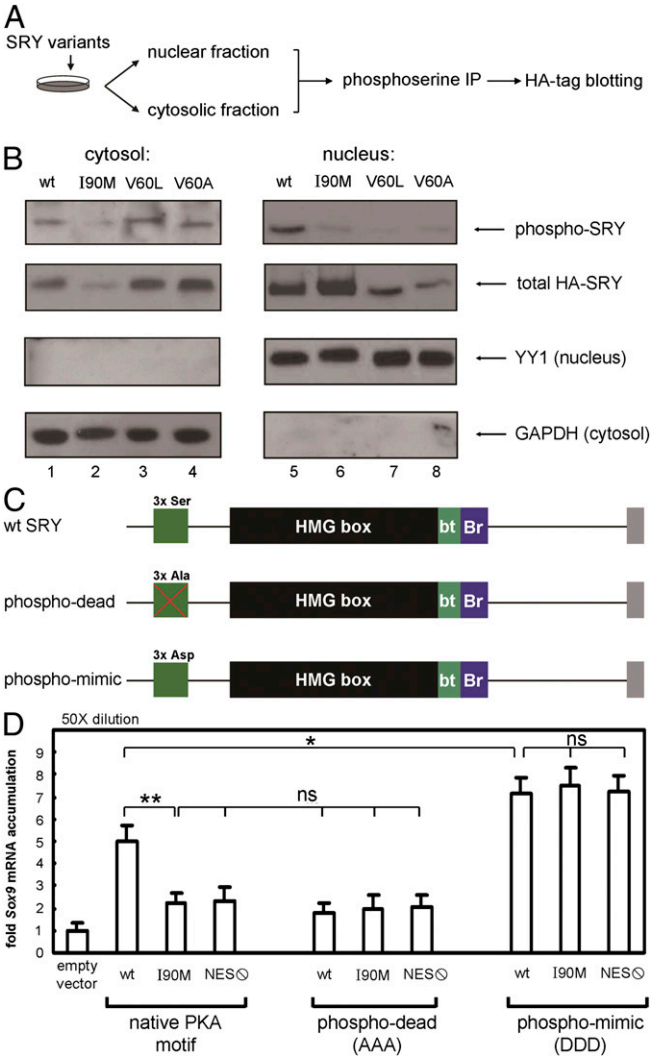

Fig. 6. Coupling between nucleocytoplasmic trafficking of hSRY and its phosphorylation. (*A*) Phosphorylation assay exploited fractionation of hSRY into nuclear and cytosolic fractions with subsequent co-IP analysis of total and phosphorylated subsets. (*B*) Western blots of cytosolic and nuclear SRY fractions (*Left* and *Right*). Mutations are as labeled; controls were provided by transcriptional repressor YY1 (nuclear protein) and GAPDH (cytosolic enzyme). (*C*) Schematic depiction of SRY analogs containing substitution within its N-terminal three contiguous PKA phosphorylation sites (PALRRSSSFLCTE; putative phosphorylation sites underlined): *Top*, WT motif; *Middle*, Ser→Ala substitutions (AAA) to render motif nonphosphorylatable (phospho-dead); *Bottom*, Ser→Asp substitutions (DDD) to mimic the negative charges (phospho-mimic). Domains are defined as in Fig. 1*A*. (*D*) Effects of AAA or DDD substitutions on transcriptional regulatory activity of WT hSRY, inherited I90M variant, or SRY NESØ in which putative NES was impaired by Ala substitutions I90A, L94A, and M100A. Studies were performed at the lowest dose used in Fig. 2. Horizontal brackets designate statistical comparisons.

in qPCR assays (Fig. 6*D*). The assays were conducted as above with 50-fold plasmid dilution and in the presence of MG132. The nonbox Ala or Asp substitutions did not affect nuclear localization (*SI Appendix*, Fig. S11) in accordance with past studies (17). WT and variant PKA sites were introduced into three epitope-tagged hSRY constructs, bearing either a WT HMG box, the I90M HMG box, or a variant HMG box in which three putative NES residues (consensus positions 35, 39, and 45) were each substituted by Ala. The latter construct (designated NESØ in Fig. 6*D*) thus yielded an hSRY variant containing six Ala substitutions, three in the nonbox PKA site (S31A, S32A, and S33A) and three in the major wing (I90A, L94A, and M100A). In the presence of the native PKA motif, I90M caused the expected twofold reduction in *Sox9* mRNA accumulation (relative to WT hSRY) as did the NESØ construct (left-hand set of bars in Fig. 6*D*). Strikingly, mimicry of PKA phosphorylation site by tandem Asp substitutions in each case led to enhanced and equal *Sox9* expression (right-hand set of bars in Fig. 6*D*). This finding provides evidence that (*i*) serine phosphorylation enhances the activity of hSRY in an appropriate cellular milieu and (*ii*) defective phosphorylation of I90M hSRY underlies its partial loss of activity. Conversely, in the phospho-dead context, WT hSRY exhibited the same twofold loss of function as was conferred by I90M or the NES Ala substitutions (middle group of bars in Fig. 6*D*). These findings suggest that unphosphorylated hSRY retains partial activity whether the defect in phosphorylation is due to mutation of the PKA site or to mutations in the HMG box that impair nuclear exit.

Extension to Human Cell Lines. In an effort to confirm a subset of key findings in a human cellular milieu, transient-transfection studies were conducted in male prostatic cell line PC-3 (41). This line expresses SF1 but not SRY. On transient transfection of the undiluted WT SRY plasmid, transcription of the endogenous *SOX9* gene was activated by fourfold (*SI Appendix*, Fig. S12). Although this fold-activity is lower than that in CH34 cells, limiting the extent of feasible plasmid dilution, transient transfection of WT or variant hSRY plasmids without dilution yielded a pattern of relative activities [*ca.* twofold decreased for V60A,L and 35(±4)% increased for I90M] that mirrored results of CH34 assays (*SI Appendix*, Fig. S12). The enhanced activity of I90M SRY on overexpression was mitigated on 20-fold dilution, consistent with our finding in CH34 cells that such enhancement is a consequence of overexpression.

Analogous studies in NT2-D1 cells [derived from a human embryonal carcinoma cell line (42) and used in cotransfection studies of SRY by Harley and coworkers (13)] were not feasible due to inefficient transcriptional activation of its endogenous SOX9 gene by transfected SRY despite its comparable overexpression. Such differences in fold-*SOX9*/*Sox9* transcriptional activation presumably reflects lineage-specific patterns of global gene expression (including other TFs and noncoding RNAs) and local chromatin structure (such as histone modifications within TES) (43).

Discussion

Metazoan development is ordinarily robust. Developmental stability in the presence of cryptic genetic variation or environmental fluctuations, known as Waddington canalization (30), has stimulated interest in biochemical mechanisms of genetic capacitors (as exemplified by heat shock proteins) (44) and topological properties of gene-regulatory networks (45). A paradigm for developmental stability is provided by the *Hox* cluster, invariant even among unrelated body plans (46). Sex is different. Metazoans exhibit an extraordinary diversity of sex-determining genes and signals, including temperature and social cues (47, 48). Intersexual phenotypes, readily obtained in model organisms (49), abound in the wild, especially in the presence of environmental endocrine disruptors (50). Further, the ubiquity of bisexual and homosexual behaviors among social mammals (including in diverse human cultures across historical epochs) poses a Darwinian paradox in relation to reproductive fitness (51).

In this study, we exploited clinical mutations in SRY associated with variable phenotypes (14, 52, 53) to measure the transcriptional threshold of testis determination. Our studies thus focused on subtle variants inherited by sterile XY daughters from fertile fathers. Potential artifacts of TF overexpression were mitigated through dilution of the hSRY expression plasmid (driven by the strong CMV promoter) by the parent empty vector to obtain a level of hSRY expression (10^2 to 10^4 molecules per cell) typical of factors that regulate cell-fate decisions (24). Molecular analysis of the clinical variants in a mammalian embryonic gonadal-ridge cell line uncovered perturbed NCS due to impaired binding of hSRY to Exp4 (V60L,A) or CRM1 (I90M). Impaired nuclear import or export is in each case associated with twofold reduction in male-pattern *Sox9* transcription and twofold enhancement of female-pattern Wnt/β-catenin signaling. These SRY variants are thus poised at a critical boundary of activity (54), highlighting the narrow margin of "decision making" in the differentiating gonadal ridge. Such twofold perturbations are analogous to syndromes of autosomal TF haploinsufficiency (55). We anticipate that this margin will be a general characteristic of inherited Swyer mutations (*SI Appendix*, Table S1) irrespective of biochemical mechanisms of perturbation.

V60L and V60A SRY retain near-native biochemical properties (Table 1). Structural accommodation of the variant side chains reflects the flexibility of the minor wing of the HMG box. To probe gene-regulatory functions, we investigated the intrinsic gene-regulatory activity of these variants following "correction" of their altered trafficking (by NLS fusion) and accelerated degradation (by proteosome inhibition). Under these conditions, occupancy of the testis-specific *Sox9* enhancer by WT or variant proteins was similar and led to near-complete double rescue of *Sox9* mRNA accumulation; native-like inhibition of Wnt/β-catenin signaling was likewise restored. I90M impairs binding of SRY to CRM1, a mediator of nuclear export (56), leading to enhanced nuclear accumulation. Although transcriptional activation of *Sox9* is increased under conditions of overexpression (in accordance with ref. 13), successive plasmid dilution unmasked a twofold defect in *Sox9* activation.

Nucleocytoplasmic Shuttling of SRY. On plasmid dilution, impaired nuclear export of I90M hSRY attenuates its gene-regulatory activity, suggesting that WT hSRY undergoes an NCS-coupled regulatory posttranslational modification. Insight may be obtained from consideration of evolutionary patterns of conservation and divergence (*SI Appendix*, Fig. S13). Among primates, SRY alleles are highly conserved and share potential N-terminal phosphorylation sites. Their HMG boxes in each case contain consensus NES sequences (IxxxLxxxxxML). The divergent boxes of rat and mouse Sry by contrast contain an unfavorable NES substitution (M→S), shown in a recent study to impair nuclear export in association with gain of a microsatellite-associated transcriptional activation domain (22). Whereas I90M (HMG position 35) occurs within α-helix 2 and perturbs packing of the major wing, the rodent substitution occurs in a loop following this α-helix and so may be better tolerated. Competence for CRM1-mediated nuclear export is maintained in goat and deer Sry, which bear NES variant IxxxLxxxxxRL. It would be of future interest to investigate these and other mammalian SRYs in relation to NCS-coupled phosphorylation.

Like SOX9, hSRY contains a PKA site N-terminal to the HMG box (17, 20). In each case, phosphorylation enhances specific DNA-binding affinity (20). We therefore hypothesized that I90M-associated impaired nuclear export perturbs this phosphorylation, which in turn attenuates *Sox9* activation—despite increased total nuclear hSRY abundance. We therefore evaluated hSRY phosphorylation following biochemical fractionation, yielding independent estimates of phospho-hSRY in the nucleus and cytoplasm. Comparative studies of "phospho-

dead" (RRAAAFL) and "phospho-mimic" (RRDDDFL) constructs verified that negative charges enhance transcriptional potency. In either context, the extent of WT or I90M hSRY-dependent *Sox9* expression is indistinguishable at reduced (phospho-dead) or elevated (phospho-mimic) levels. Because divergent rodent Sry proteins lack this N-terminal PKA site, we speculate that its C-terminal glutamine-rich expansion provides an alternative mechanism to enhance *Sox9* transcription [see also ref. 22].

Coupling between NCS and posttranslational modification occurs in diverse systems (19, 20). Such coupling may be a hallmark of mammalian Sox proteins (19, 57) as exemplified by SOX9, which contains two PKA sites, one N-terminal to the HMG box and the other adjoining NLS2 in its C-terminal tail. The latter phosphorylation enhances NLS2 binding to importin-β and therefore promotes nuclear import (20). Autocrine regulation of PKA activity by prostaglandin D2 in the differentiating Sertoli cell may provide a mechanism to amplify and maintain *Sox9* expression as shown in engineered mice (34). Although phosphorylation-regulated nuclear localization is not a feature of hSRY, its acetylation (K136 in NLS2) provides an alternative mechanism to enhance binding to importin-β (58).

Mouse Sry Exhibits an Analogous Threshold. The inherited Swyer syndrome resembles Y-chromosome incompatibility among mouse strains wherein Y chromosomes bearing *Sry* alleles derived from diverse mouse strains can cause abnormal gonadal development in B6 strain C57BL/6J (27, 28). Aberrant interaction between such alleles and autosomal genes leads to strain-dependent intersexual phenotypes (59). Such phenotypes could not be correlated with changes in Sry sequence (28) but instead depend on the extent and timing of *Sry* expression (27, 28). As found here, changes of twofold or less in *Sry* expression in the differentiating gonadal ridge were associated with developmental abnormalities. Such genetic-background dependence strongly suggests that Sry-*Sox9*-directed transcriptional program in mice lies close to a threshold of function.

The tenuous biochemical thresholds of SRY function in mice and humans—mammals with otherwise divergent *SRY*/*Sry* genes (28)—demonstrate that lack of robustness in nascent Sertoli-cell specification has been independently maintained in lineages separated by 80 million y. Such conservation seems to violate Waddington's Principle: that fundamental developmental pathways are canalized, at least in their upstream steps, and so robust (30, 31). It is possible that the apparent fragility of hSRY is illusory. The transcriptional set point of hSRY, for example, may be so tightly controlled by upstream factors (such as GATA4 and WT1) (60) and transcriptional coregulators (such as SF1 in sex-specific transcriptional preinitiation complexes) (7) that twofold reductions in hSRY-directed *SOX9* activation would be unlikely. Similarly, it is possible that variation in hSRY activity is buffered by feedback and feed-forward regulatory circuits in the SOX9-directed gene-regulatory network (34).

Multilevel Selection in Mammalian Evolution? The similar transcriptional thresholds of murine and human SRY [despite their biochemical divergence; see a recent study (22)] suggests that its thin thread of function (29) is the product of selection. The shared tenuousness of the switch poses an intriguing problem given the general robustness of developmental processes (61). It is possible that an hSRY of higher transcriptional potency could impair individual fitness, such as through induction of gonadal neoplasias (13). Alternatively, higher potency could lead to intragenomic conflict with female-specific genes and so impair daughter fitness (62). Genes that contribute to variation in male-specific traits, including hormone-dependent behaviors and social competencies[§] (63), may also be subject to intrasexual selection (such as in male dominance hierarchies) or intersexual selection (female mate choice) (64).

We speculate that genetic variation in fetal testosterone production influenced the evolution of eutherian mammals, especially species (like humans and mice) that evolved within social groups. Given epidemiological linkages between human fetal testosterone exposure (as measured in midtrimester amniotic fluid) and behavioral styles in childhood (65), it is possible that genetic or stochastic variation in fetal Leydig-cell function could ultimately affect mate choice, reproductive success, or social integration within the framework of multilevel selection (66). Indeed, nonrobustness is a hallmark of human genetics at successive stages of male differentiation (67). Heterozygous nonsense and missense mutations in SF1 associated with gonadal dysgenesis likewise suggest (in the absence of adrenal abnormalities) a syndrome of haploinsufficiency (68, 69). Mutations in *SOX9*, moreover, result in a syndrome of TF haploinsufficiency (campomelic dysplasia), wherein abnormalities of bone coincide (in XY patients) with male, intersex, or female somatic phenotypes (70). Such phenotypic variability suggests that the twofold transcriptional threshold characteristic of hSRY extends to its immediate downstream target. Similarly, hemizygosity of chromosome 9p24.3 (which contains three *DM* genes related to the *Doublesex* gene of *Dipterans*) (71) is associated with 46,XY gonadal dysgenesis in the presence of WT *SRY* and *SOX9* alleles (72). This trend extends to the androgen receptor itself. Studies of the X-linked androgen insensitivity syndrome have demonstrated that the same receptor mutation can be associated with complete feminization ("testicular feminization"), partial insensitivity, or minimal perturbations in virilization or fertility[¶] (73). Together, these clinical entities highlight the anomalous nonrobustness of the male program.

Concluding Remarks. Our studies address an overarching issue in human development: biochemical properties of TFs that distinguish critical boundaries between organized and disorganized states of cellular differentiation or downstream pathways of pattern formation (54). Inherited alleles of *SRY* provide probes of this boundary in gonadogenesis. Our results, demonstrating that NCS and NCS-coupled phosphorylation of hSRY contribute at the margin to its genetic function, highlight the tenuous transcriptional threshold of human Sertoli-cell specification. A similar threshold pertains to testicular differentiation in mice (11) despite the marked biochemical divergence of murine Sry (22).

Given general trends toward the evolution of developmental stability (30), why have human and murine SRY evolved to the edge of ambiguity? We speculate that sex determination differs from canonical embryonic patterning through its coupling to variation in extent of testosterone secretion by fetal Leydig cells, in turn enabling male neurodevelopmental diversity. This perspective highlights the complementary and potentially conflicting roles of within-group and between-group selection as a feature of multilevel selection in social mammals (66). Implicit in this view are connections between genotype, development, differentiation of the central nervous system, and complex behaviors, including empathy and other social competencies as defined in longitudinal studies of human fetal testosterone exposure (65). A connection between multilevel selection and social competencies was anticipated by Darwin's surmise that "although a high standard of morality gives but a slight or no advantage to each individual man and his children over the other men of the same tribe,... an increase in the number of well-endowed men and advancement in the standard of morality will certainly give an

[§]Positioning of XX and XY fetuses in litter-bearing mammals influences local testosterone concentrations and thus postnatal reproductive traits, including timing of puberty, sexual behaviors, and aggressiveness (75).

[¶]Instructive examples are provided by mutations R840C and R840H in the ligand-binding domain of the androgen receptor (76–78). These mutations are associated with a broad spectrum of partial phenotypes ranging from micropenis (Reifenstein syndrome with patient raised as male) to external female genitalia (incomplete testicular feminization with patient raised as female). Biochemical affinities of the variant domains for testosterone are reduced by less than fourfold.

immense advantage to one tribe over another" (66, 74). The anomalous nonrobustness of male sex determination and sexual differentiation in social mammals, as evidenced by inherited alleles of human *SRY* at the edge of ambiguity, may relate Darwin's insight to the tenuous biochemistry of a genetic switch.

Materials and Methods

Plasmids. Plasmids expressing hSRY or variants were constructed by PCR (14). Following the initiator methionine, the cloning site encoded an HA tag in triplicate. In selected constructs, an element encoding a nuclear localization signal (NLS) sequence PRRRKV as derived from SV40 large T antigen was inserted after HA-related codons.

Cell Culture. CH34 cells were cultured in Dulbecco's modified Eagle medium as described (14). For proteasome-inhibitor studies, transfected cells were maintained for 24 h in serum-free conditions and then treated with MG132 for 6 h followed by 18 h incubation in 5% (vol/vol) serum-containing medium. PC-3 cells were cultured in the F-12K medium (ATCC) with 10% (vol/vol) FBS in 5% CO_2 atmosphere. NT2-D1 cells were grown in DMEM in an atmosphere of 5% CO_2; the complete growth medium contained FBS to a final concentration of 10%. SOX9- and TBP-specific PCR primers were in accordance with human genomic sequences.

Transient Transfection. Transfections were performed as described (14). Transfection efficiencies (30–35% in the case of CH34 cells) were determined by ratio of GFP-positive cells to untransfected cells following cotransfection with pCMX-SRY and pCMX-GFP in equal amounts. Subcellular localization was visualized by immunostaining 24 h posttransfection following treatment with 0.01% trypsin (Invitrogen) and plating on 12-mm coverslips. SRY expression was monitored in triplicate by Western blot in relation to α-tubulin (*SI Appendix*, Fig. S14).

Cycloheximide-Chase Assay and Western Blot. Twenty-four hours posttransfection, cells were split evenly into six-well plates and treated with cycloheximide to a final concentration of 20 mg/mL in regular medium for indicated times; cells were then lysed by radio immunoprecipitation assay (RIPA) buffer (Hoffmann LaRoche). After protein normalization, cell lysates were subjected to 12% SDS/PAGE and Western blot using anti-HA antiserum (Sigma-Aldrich) at a dilution ratio of 1:5,000 with α-tubulin as a loading control. Experiments were performed in triplicate.

***Sox9* Activation Assay.** SRY-mediated transcriptional activation of *Sox9* and other endogenous CH34 genes was measured in triplicate by qPCR as described (14). Cellular RNA was extracted using RNeasy (Qiagen).

Immunocytochemistry. Transfected cells were plated evenly on 12-mm coverslips, fixed with 3% *para*-formaldehyde in PBS on ice for 30 min, treated with cold-permeability buffer solution (PBS containing 10% goat serum and 1% Triton X-100; Sigma-Aldrich) for 10 min, blocked with 10% goat serum and 0.1% Tween 20 in cold PBS (Sigma-Aldrich), and incubated overnight at 4 °C with FITC-conjugated anti-HA antibody (diluted to 1:400 ratio; Santa Cruz). After washing and DAPI staining, cells were visualized by fluorescent microscopy. Nuclear localization was evaluated by the ratio of SRY detected in nucleus to the total number of GFP-positive cells; 800–1,000 cells were counted in each case.

Chromatin Immunoprecipitation. Cells were transfected with SRY variants, exposed to MG132, and subjected to ChIP. In brief, recovered cells were cross-linked in wells by formaldehyde, collected, and lysed after quenching the cross-linking reaction. Chromatin lysates were sonicated to generate 300- to 400-bp fragments and immunoprecipitated with anti-HA antiserum (Sigma-Aldrich) coupled with Protein A slurry (Santa Cruz) after preclearing; a nonspecific antiserum (Santa Cruz) served as control. After reversal of cross-linking at 65 °C overnight, fragments were treated with proteinase K and RNase (Hoffmann LaRoche), followed by extraction with 1:1 phenol-CIAA solution. A high-fidelity PCR protocol was provided by Hoffmann LaRoche. Experiments were performed in triplicate.

Phosphorylation Assay. HA-tagged SRY variants in cytosolic or nuclear fractions (below) were immunoprecipitated with rabbit polyclonal anti-phosphoserine antiserum (Abcam). Western blot following 12% SDS/PAGE used HRP-conjugated anti-HA antibody (Hoffmann LaRoche). Loading controls were provided by cytosolic enzyme GAPDH (Sigma-Aldrich) and nuclear proteins histone H1 and YY1 (Santa Cruz).

Wnt/β-Catenin Luciferase Assay. CH34 cells were engineered to stably express S37A β-catenin as described (39). Assays, adapted from previous studies (39), used a chimeric SRY containing residues 1–155 of hSRY followed by residues 128–396 of mouse Sry. Experiments were conducted in triplicate using the Dual-Luciferase Reporter Assay System (Promega); lysates were simultaneously analyzed for firefly luciferase activity encoded by TOPflash (Millipore) and *Renilla* luciferase activity (Promega). A negative control for β-catenin–directed luciferase expression was provided by a TOPflash variant containing an inactive β-catenin–responsive promoter (FOPflash; Millipore). Experiments were performed in triplicate.

Coimmunoprecipitation Assays. CH34 cells expressing HA-tagged SRY variants were treated with MG132 and lysed using complete Lysis-M buffer containing a protease inhibitor mixture (Hoffmann LaRoche). In SRY–CaM studies, lysates were precipitated with monoclonal anti-HA agarose beads (Sigma-Aldrich). Following 12% SDS/PAGE, Western blots used an anti-CaM antiserum (Abcam). In SRY–CRM1 studies, lysates were analyzed by immunoprecipitation using anti-CRM1 antibody with agarose-conjugated protein G (Santa Cruz). Pellets were subjected to 10% SDS/PAGE, and HRP-conjugated anti-HA antiserum (Hoffmann LaRoche) was used to investigate the CRM1-bound HA-SRY variants. In a reverse protocol, lysates were treated with monoclonal agarose-conjugated anti-HA antiserum (Sigma-Aldrich), subjected to 10% SDS/PAGE electrophoresis, and analyzed by anti-CRM1 antibody (Santa Cruz) to detect SRY-bounded CRM1. In SRY–Exp4 studies, transfected cells were cotransfected with pCMX-FLAG-human Exp4. MG132-treated cell lysates were immunoprecipitated by monoclonal anti-FLAG agarose (Sigma-Aldrich). After analysis by 10% SDS/PAGE and electroblotting, hybridization solutions containing HRP-conjugated anti-HA antiserum (Hoffmann LaRoche) were used to investigate Exp4-bound SRY. Anti-FLAG antiserum was used to monitor Exp4 expression; respective antisera against HA tag and α-tubulin (Sigma-Aldrich) provided SRY input- and general loading controls.

Cellular Fractionation. Cells were pelleted and suspended in 10 mM Hepes (pH 7.9), 20 mM KCl, 3mM $MgCl_2$, 0.5% Nonidet P-40, 5% glycerol, 10 μg/mL leupeptin, 10 μg/mL aprotinin, and 1 mM phenylmethylsulfonyl fluoride (Sigma-Aldrich). Lysates were kept on ice, sheared by five passages through a 25-gauge needle, and centrifuged at 2,500 × *g* for 15 min at 4 °C; supernatants provided cytosolic extract. Pellets were suspended in nuclear lysis buffer [20 mM Hepes (pH 7.9), 0.225 M NaCl, 1 mM EDTA, 3 mM $MgCl_2$, 0.5% Nonidet P-40, 10% glycerol, 10 μg/mL leupeptin, 10 μg/mL aprotinin, and 1 mM phenylmethylsulfonyl fluoride], sheared by needle passage, kept on ice for 15 min, and subjected to 13,000 × *g* centrifugation for 15 min at 4 °C.

ACKNOWLEDGMENTS. We thank Prof. P. K. Donahoe for cell line CH34 and encouragement; P. Janki and S. Jeong for assistance; T. Feng, B. Li, and R. Singh for participation in early stages of this work; and P. DeHaseth, H.-Y. Kao, D. Samols, and P. Sequeira for advice. M.A.W. thanks B. Baker, F. A. Jenkins, Jr., and P. Koopman for discussion. This work was supported in part by National Institutes of Health Grant GM080505 (to M.A.W.). This article is dedicated to the memory of the late Prof. Farish A. Jenkins, Jr. (Harvard University and the Harvard-MIT Program in Health Sciences and Technology) for his encouragement, humanity, and scientific example.

1. Sinclair AH, et al. (1990) A gene from the human sex-determining region encodes a protein with homology to a conserved DNA-binding motif. *Nature* 346(6281): 240–244.
2. Sekido R (2010) SRY: A transcriptional activator of mammalian testis determination. *Int J Biochem Cell Biol* 42(3):417–420.
3. Ner SS (1992) HMGs everywhere. *Curr Biol* 2(4):208–210.
4. King CY, Weiss MA (1993) The SRY high-mobility-group box recognizes DNA by partial intercalation in the minor groove: A topological mechanism of sequence specificity. *Proc Natl Acad Sci USA* 90(24):11990–11994.
5. Koopman P, Gubbay J, Vivian N, Goodfellow P, Lovell-Badge R (1991) Male development of chromosomally female mice transgenic for Sry. *Nature* 351(6322): 117–121.
6. Knower KC, Kelly S, Harley VR (2003) Turning on the male—SRY, SOX9 and sex determination in mammals. *Cytogenet Genome Res* 101(3-4):185–198.
7. Sekido R, Lovell-Badge R (2008) Sex determination involves synergistic action of SRY and SF1 on a specific *Sox9* enhancer. *Nature* 453(7197):930–934.
8. Lovell-Badge R, Canning C, Sekido R (2002) *Sex-Determining Genes in Mice: Building Pathways* (Wiley, West Sussex, UK), pp 4–22.

9. Josso N, Picard JY, Rey R, di Clemente N (2006) Testicular anti-Müllerian hormone: History, genetics, regulation and clinical applications. *Pediatr Endocrinol Rev* 3(4): 347–358.
10. McClelland K, Bowles J, Koopman P (2012) Male sex determination: Insights into molecular mechanisms. *Asian J Androl* 14(1):164–171.
11. Wilhelm D, Koopman P (2006) The makings of maleness: Towards an integrated view of male sexual development. *Nat Rev Genet* 7(8):620–631.
12. Murphy EC, Zhurkin VB, Louis JM, Cornilescu G, Clore GM (2001) Structural basis for SRY-dependent 46-X,Y sex reversal: Modulation of DNA bending by a naturally occurring point mutation. *J Mol Biol* 312(3):481–499.
13. Knower KC, et al. (2011) Failure of SOX9 regulation in 46XY disorders of sex development with SRY, SOX9 and SF1 mutations. *PLoS ONE* 6(3):e17751.
14. Phillips NB, et al. (2011) Mammilian testis-determining factor SRY and the enigma of inherited human sex reversal. *J Biol Chem* 286:36787–36807.
15. Haqq CM, et al. (1994) Molecular basis of mammalian sexual determination: Activation of Müllerian inhibiting substance gene expression by SRY. *Science* 266(5190):1494–1500.
16. Haqq CM, Donahoe PK (1998) Regulation of sexual dimorphism in mammals. *Physiol Rev* 78(1):1–33.
17. Desclozeaux M, et al. (1998) Phosphorylation of an N-terminal motif enhances DNA-binding activity of the human SRY protein. *J Biol Chem* 273(14):7988–7995.
18. Malki S, et al. (2005) Prostaglandin D2 induces nuclear import of the sex-determining factor SOX9 via its cAMP-PKA phosphorylation. *EMBO J* 24(10):1798–1809.
19. Malki S, Boizet-Bonhoure B, Poulat F (2010) Shuttling of SOX proteins. *Int J Biochem Cell Biol* 42(3):411–416.
20. Sim H, Argentaro A, Harley VR (2008) Boys, girls and shuttling of SRY and SOX9. *Trends Endocrinol Metab* 19(6):213–222.
21. Poulat F, et al. (1995) Nuclear localization of the testis determining gene product SRY. *J Cell Biol* 128(5):737–748.
22. Chen YS, Racca JD, Sequeira PW, Phillips NB, Weiss MA (2013) Microsatellite-encoded domain in rodent Sry functions as a genetic capacitor to enable the rapid evolution of biological novelty. *Proc Natl Acad Sci USA* 110(33):E3061–E3070.
23. Bowles J, Cooper L, Berkman J, Koopman P (1999) Sry requires a CAG repeat domain for male sex determination in Mus musculus. *Nat Genet* 22(4):405–408.
24. Goentoro L, Shoval O, Kirschner MW, Alon U (2009) The incoherent feedforward loop can provide fold-change detection in gene regulation. *Mol Cell* 36(5):894–899.
25. Qin JY, et al. (2010) Systematic comparison of constitutive promoters and the doxycycline-inducible promoter. *PLoS ONE* 5(5):e10611.
26. Niwa H, Miyazaki J, Smith AG (2000) Quantitative expression of Oct-3/4 defines differentiation, dedifferentiation or self-renewal of ES cells. *Nat Genet* 24(4):372–376.
27. Albrecht KH, Young M, Washburn LL, Eicher EM (2003) *Sry* expression level and protein isoform differences play a role in abnormal testis development in C57BL/6J mice carrying certain *Sry* alleles. *Genetics* 164(1):277–288.
28. Bullejos M, Koopman P (2005) Delayed *Sry* and *Sox9* expression in developing mouse gonads underlies B6-Y(^{DOM}) sex reversal. *Dev Biol* 278(2):473–481.
29. Polanco JC, Koopman P (2007) Sry and the hesitant beginnings of male development. *Dev Biol* 302(1):13–24.
30. Waddington CH (1959) Canalization of development and genetic assimilation of acquired characters. *Nature* 183(4676):1654–1655.
31. Masel J, Siegal ML (2009) Robustness: Mechanisms and consequences. *Trends Genet* 25(9):395–403.
32. Koopman P, Bullejos M, Bowles J (2001) Regulation of male sexual development by Sry and Sox9. *J Exp Zool* 290(5):463–474.
33. Hiort O, Gramss B, Klauber GT (1995) True hermaphroditism with 46,XY karyotype and a point mutation in the SRY gene. *J Pediatr* 126(6):1022.
34. Moniot B, et al. (2009) The PGD2 pathway, independently of FGF9, amplifies SOX9 activity in Sertoli cells during male sexual differentiation. *Development* 136(11): 1813–1821.
35. Weiss MA, Ukiyama E, King CY (1997) The SRY cantilever motif discriminates between sequence- and structure-specific DNA recognition: Alanine mutagenesis of an HMG box. *J Biomol Struct Dyn* 15(2):177–184.
36. Kalderon D, Roberts BL, Richardson WD, Smith AE (1984) A short amino acid sequence able to specify nuclear location. *Cell* 39(3 Pt 2):499–509.
37. Gontan C, et al. (2009) Exportin 4 mediates a novel nuclear import pathway for Sox family transcription factors. *J Cell Biol* 185(1):27–34.
38. Sim H, et al. (2005) Defective calmodulin-mediated nuclear transport of the sex-determining region of the Y chromosome (SRY) in XY sex reversal. *Mol Endocrinol* 19(7):1884–1892.
39. Bernard P, Sim H, Knower K, Vilain E, Harley V (2008) Human SRY inhibits β-catenin-mediated transcription. *Int J Biochem Cell Biol* 40(12):2889–2900.
40. Maatouk DM, et al. (2008) Stabilization of β-catenin in XY gonads causes male-to-female sex-reversal. *Hum Mol Genet* 17(19):2949–2955.
41. Kaighn ME, Narayan KS, Ohnuki Y, Lechner JF, Jones LW (1979) Establishment and characterization of a human prostatic carcinoma cell line (PC-3). *Invest Urol* 17(1): 16–23.
42. Knower KC, et al. (2007) Characterisation of urogenital ridge gene expression in the human embryonal carcinoma cell line NT2/D1. *Sex Dev* 1(2):114–126.
43. Sproul D, Gilbert N, Bickmore WA (2005) The role of chromatin structure in regulating the expression of clustered genes. *Nat Rev Genet* 6(10):775–781.
44. Rutherford SL, Lindquist S (1998) Hsp90 as a capacitor for morphological evolution. *Nature* 396(6709):336–342.
45. Siegal ML, Promislow DE, Bergman A (2007) Functional and evolutionary inference in gene networks: Does topology matter? *Genetica* 129(1):83–103.
46. Barmina O, Kopp A (2007) Sex-specific expression of a HOX gene associated with rapid morphological evolution. *Dev Biol* 311(2):277–286.
47. Rhen T, Crews D (1999) Embryonic temperature and gonadal sex organize male-typical sexual and aggressive behavior in a lizard with temperature-dependent sex determination. *Endocrinology* 140(10):4501–4508.
48. Kobayashi Y, et al. (2009) Sex change in the Gobiid fish is mediated through rapid switching of gonadotropin receptors from ovarian to testicular portion or vice versa. *Endocrinology* 150(3):1503–1511.
49. Baker ME (2011) Insights from the structure of estrogen receptor into the evolution of estrogens: Implications for endocrine disruption. *Biochem Pharmacol* 82(1):1–8.
50. Storrs-Méndez SI, Semlitsch RD (2010) Intersex gonads in frogs: Understanding the time course of natural development and role of endocrine disruptors. *J Exp Zoolog B Mol Dev Evol* 314(1):57–66.
51. Jannini EA, Blanchard R, Camperio-Ciani A, Bancroft J (2010) Male homosexuality: Nature or culture? *J Sex Med* 7(10):3245–3253.
52. Jäger RJ, Harley VR, Pfeiffer RA, Goodfellow PN, Scherer G (1992) A familial mutation in the testis-determining gene SRY shared by both sexes. *Hum Genet* 90(4):350–355.
53. Harley VR, et al. (1992) DNA binding activity of recombinant SRY from normal males and XY females. *Science* 255(5043):453–456.
54. Nykter M, et al. (2008) Gene expression dynamics in the macrophage exhibit criticality. *Proc Natl Acad Sci USA* 105(6):1897–1900.
55. Seidman JG, Seidman C (2002) Transcription factor haploinsufficiency: When half a loaf is not enough. *J Clin Invest* 109(4):451–455.
56. Fornerod M, Ohno M, Yoshida M, Mattaj IW (1997) CRM1 is an export receptor for leucine-rich nuclear export signals. *Cell* 90(6):1051–1060.
57. Smith JM, Koopman PA (2004) The ins and outs of transcriptional control: Nucleocytoplasmic shuttling in development and disease. *Trends Genet* 20(1):4–8.
58. Thevenet L, et al. (2004) Regulation of human SRY subcellular distribution by its acetylation/deacetylation. *EMBO J* 23(16):3336–3345.
59. Nagamine CM, Taketo T, Koo GC (1987) Morphological development of the mouse gonad in tda-1 XY sex reversal. *Differentiation* 33(3):214–222.
60. Miyamoto Y, Taniguchi H, Hamel F, Silversides DW, Viger RS (2008) A GATA4/WT1 cooperation regulates transcription of genes required for mammalian sex determination and differentiation. *BMC Mol Biol* 9:44.
61. Siegal ML, Bergman A (2002) Waddington's canalization revisited: Developmental stability and evolution. *Proc Natl Acad Sci USA* 99(16):10528–10532.
62. Gibson JR, Chippindale AK, Rice WR (2002) The X chromosome is a hot spot for sexually antagonistic fitness variation. *Proc Biol Sci* 269(1490):499–505.
63. vom Saal FS (1981) Variation in phenotype due to random intrauterine positioning of male and female fetuses in rodents. *J Reprod Fertil* 62(2):633–650.
64. Civetta A, Singh RS (1998) Sex-related genes, directional sexual selection, and speciation. *Mol Biol Evol* 15(7):901–909.
65. Baron-Cohen S, Lutchmaya S, Knickmeyer R (2004) *Prenatal Testosterone in Mind: Amniotic Fluid Studies* (MIT Press, Cambridge, MA), p 141.
66. Wilson DS, Wilson EO (2007) Rethinking the theoretical foundation of sociobiology. *Q Rev Biol* 82(4):327–348.
67. Huang B, Wang S, Ning Y, Lamb AN, Bartley J (1999) Autosomal XX sex reversal caused by duplication of SOX9. *Am J Med Genet* 87(4):349–353.
68. Mallet D, et al. (2004) Gonadal dysgenesis without adrenal insufficiency in a 46, XY patient heterozygous for the nonsense C16X mutation: A case of SF1 haploinsufficiency. *J Clin Endocrinol Metab* 89(10):4829–4832.
69. Lin L, et al. (2007) Heterozygous missense mutations in steroidogenic factor 1 (SF1/Ad4BP, NR5A1) are associated with 46,XY disorders of sex development with normal adrenal function. *J Clin Endocrinol Metab* 92(3):991–999.
70. Baek WY, Kim JE (2011) Transcriptional regulation of bone formation. *Front Biosci (Schol Ed)* 3:126–135.
71. Raymond CS, et al. (1998) Evidence for evolutionary conservation of sex-determining genes. *Nature* 391(6668):691–695.
72. Barbaro M, et al. (2009) Characterization of deletions at 9p affecting the candidate regions for sex reversal and deletion 9p syndrome by MLPA. *Eur J Hum Genet* 17(11): 1439–1447.
73. Bennett NC, Gardiner RA, Hooper JD, Johnson DW, Gobe GC (2010) Molecular cell biology of androgen receptor signalling. *Int J Biochem Cell Biol* 42(6):813–827.
74. Darwin C (1871) *The Descent of Man, and Selection in Relation to Sex* (Appleton, New York), Vols 1 and 2.
75. vom Saal FS (1989) Sexual differentiation in litter-bearing mammals: Influence of sex of adjacent fetuses in utero. *J Anim Sci* 67(7):1824–1840.
76. Marcelli M, Zoppi S, Wilson CM, Griffin JE, McPhaul MJ (1994) Amino acid substitutions in the hormone-binding domain of the human androgen receptor alter the stability of the hormone receptor complex. *J Clin Invest* 94(4):1642–1650.
77. Evans BAJ, Hughes IA, Bevan CL, Patterson MN, Gregory JW (1997) Phenotypic diversity in siblings with partial androgen insensitivity syndrome. *Arch Dis Child* 76(6): 529–531.
78. Chu J, et al. (2002) Male fertility is compatible with an Arg^{840}Cys substitution in the AR in a large Chinese family affected with divergent phenotypes of AR insensitivity syndrome. *J Clin Endocrinol Metab* 87(1):347–351.